

Analytic Method of 3-D Foundation-Structure System With the Viscous Boundaries Considering the Vertical Motion



Z. Cao

JP Business Service Corporation, Japan

A. Saotome

Electric Power Development Co., Ltd., Japan

SUMMARY

For the dynamic analyses of 3-D foundation-structure systems, a viscous boundary condition based on the principle of virtual work was proposed by Miura F., in 1989. It has been proved to be much more effective for absorbing the scattered waves than the traditional viscous boundaries. However, it was based on the assumption of horizontal earthquake motion and the proposed bottom viscous boundary could not give a satisfied solution because the definition of the earthquake input with the bottom viscous boundary was not clear. Therefore, in this study, the analytic method proposed by Miura is modified for corresponding to 3-D earthquake response problems. The formulations of the motion equations of the foundation-structure system and the earthquake input method are presented with the bottom viscous boundary and improved lateral boundary conditions. Moreover, for precisely considering the effects of the displacement of the free fields, the stiffness matrices of the lateral boundaries are modified to correspond to both the horizontal and vertical earthquake motions. Finally, the validation of the modified method proposed in the study is examined by a verification analysis.

Keywords: foundation-structure system, viscous boundary, vertical motion, three dimensional analysis

1. INTRODUCTION

The recent strong earthquakes, such as the 2011 Tohoku Earthquake and the 1995 Hyogo-ken Nanbu Earthquake show the common characteristic of strong vertical motion. How to consider the effects of the vertical earthquake motion in the designs of structures and foundations has become one of the serious problems we have to face. For instance, for the earthquake resistant design or seismic assessment of the electric power plants, the hybrid method of the dynamic analysis for horizontal earthquake motion and the quasi-static analysis for vertical motion has being applied up to now. Recently active researches about the effects of vertical motion on the safety of the power plant structures have been in progress. On the other hand, the 3-D linear and nonlinear FEM analysis of foundation - structures has been being applied practically.

In the 3-D FEM analysis of the foundation-structures, an imperative problem is how to set the boundary conditions of the numerical model for considering the effects of free fields. In the early 1990's, Miura proposed a viscous boundary condition for absorbing the scattered waves that occurred within the foundation - structure system and the irregular shaped foundation. This method also can take the effects of free field motion into consideration. It has been verified to be much more effective than the traditional viscous boundary proposed by Lysmer in 1972. However, the study of Miura was based on the assumption of horizontal earthquake motion, and it was concluded that for the bottom boundary of the foundation, the fixed condition is somewhat better than the viscous one. In fact, the imperfect definition of the earthquake input with a bottom viscous boundary misled the result. Therefore the original method proposed by Miura was deficient for the analyses of vertical earthquake motion or when the bottom viscous boundary condition is necessary. Concretely, it is necessary to improve the original method on the following two problems.

- 1) In the case that the vertical earthquake motion is predominant or the reflection of the scattered waves at the bottom boundary is supposed, the bottom boundary condition should have the

function of absorbing the scattered waves and a proper formulation of the earthquake input should be defined concurrently.

- 2) In the case of 3 directional earthquake input, the traction force acting on the lateral boundaries of the foundation due to the phase difference between the foundation and the free field should be calculated with the consideration of 3 directional earthquake motions simultaneously.

For solving the problems mentioned above, the method proposed by Miura is improved by extending the stiffness and viscous matrices of the lateral boundaries into 3-D formation. The FEM formulation of the motion equations and the earthquake input definition have been given when the bottom viscous boundary is applied. Then, an analysis has been done for verifying the improved method. It has been concluded that the improved method has a sufficient function for practical engineering application.

In this paper, the theoretical derivation has to be abridged because of the space limitation. If necessary, referring the paper of Miura is recommended.

2. BOTTOM VISCOUS BOUNDARY AND CORRESPONDING EARTHQUAKE INPUT

Here the definition of the viscous boundary condition on the foundation bottom is given.

Based on the multiple reflection theory, the earthquake input through the foundation bottom with the viscous boundary condition can be expressed as the following form

$$\{F_e\} = [C]_{BS} (\{\dot{z}\} - \{\dot{u}\}) \quad (2.1)$$

where, $\{F_e\}$ is the earthquake load on the foundation bottom, $[C]_{BS}$ is the viscous boundary matrix, $\{\dot{z}\}$ and $\{\dot{u}\}$ respectively represent the ground earthquake velocity vector and the velocity response vector of the nodes on the foundation bottom.

As shown in Fig. 2.1, the 2E components of the primary wave and shear wave are input beneath the bottom viscous boundary, symbolized as $\{\dot{z}\}$. The bottom viscous boundary should have double functions. It should let the upward transmitting wave (E) pass through it, and simultaneously absorb the downward transmitting wave (F). With the same theoretic derivation as Miura did, the matrix $[C]_{BS}$ of a rectangular element can be expressed as the following form

$$[C]_{BS} = \frac{\rho d}{36} \begin{bmatrix} 4V_s & 0 & 0 & 2V_s & 0 & 0 & V_s & 0 & 0 & 2V_s & 0 & 0 \\ 0 & 4V_s & 0 & 0 & 2V_s & 0 & 0 & V_s & 0 & 0 & 2V_s & 0 \\ 0 & 0 & 4V_p & 0 & 0 & 2V_p & 0 & 0 & V_p & 0 & 0 & 2V_p \\ 2V_s & 0 & 0 & 4V_s & 0 & 0 & 2V_s & 0 & 0 & V_s & 0 & 0 \\ 0 & 2V_s & 0 & 0 & 4V_s & 0 & 0 & 2V_s & 0 & 0 & V_s & 0 \\ 0 & 0 & 2V_p & 0 & 0 & 4V_p & 0 & 0 & 2V_p & 0 & 0 & V_p \\ V_s & 0 & 0 & 2V_s & 0 & 0 & 4V_s & 0 & 0 & 2V_s & 0 & 0 \\ 0 & V_s & 0 & 0 & 2V_s & 0 & 0 & 4V_s & 0 & 0 & 2V_s & 0 \\ 0 & 0 & V_p & 0 & 0 & 2V_p & 0 & 0 & 4V_p & 0 & 0 & 2V_p \\ 2V_s & 0 & 0 & V_s & 0 & 0 & 2V_s & 0 & 0 & 4V_s & 0 & 0 \\ 0 & 2V_s & 0 & 0 & V_s & 0 & 0 & 2V_s & 0 & 0 & 4V_s & 0 \\ 0 & 0 & 2V_p & 0 & 0 & V_p & 0 & 0 & 2V_p & 0 & 0 & 4V_p \end{bmatrix}$$

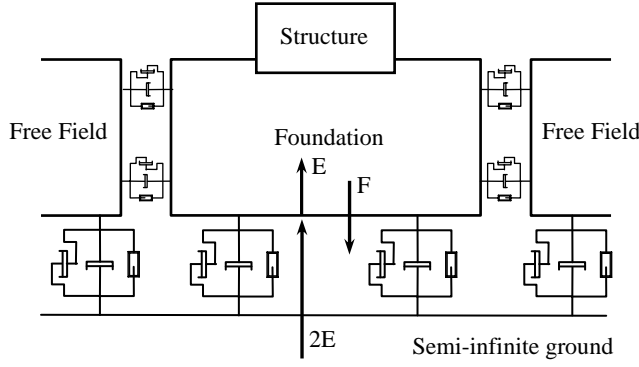


Figure.2.1 Bottom viscous boundary and earthquake input

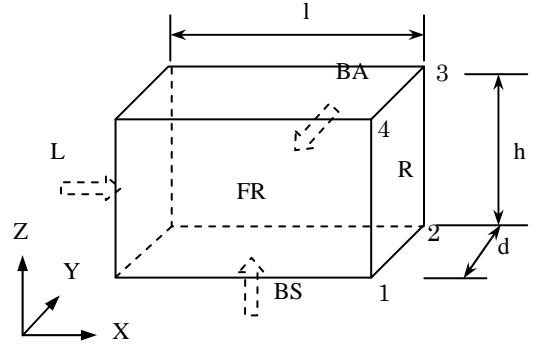


Figure 2.2 Name of the boundary surfaces

where ρ is the density of the foundation, l and d are the length and width of the element of the bottom boundary respectively as shown in Fig.2.2. V_s and V_p are the velocities of shear wave and primary wave respectively.

For the numerical model with bottom viscous boundary, the earthquake load acting on the bottom surface is defined by Eqn. 2.1, and the motion equation of the foundation-structure system can be expressed as the following form

$$\begin{aligned}
& [M]\{\ddot{u}\} + ([C] + [C]_{BS} + [C]_{FR} + [C]_{BA} + [C]_L + [C]_R)\{\dot{u}\} + [K]\{u\} \\
& = [C]_{BS}\{\dot{z}\} + [G]_{FR}\{u^f\}_{FR} + [G]_{BA}\{u^f\}_{BA} + [G]_L\{u^f\}_L + [G]_R\{u^f\}_R \\
& + ([G_C]_{FR} + [C]_{FR})\{\dot{u}^f\}_{FR} + ([G_C]_{BA} + [C]_{BA})\{\dot{u}^f\}_{BA} \\
& + ([G_C]_L + [C]_L)\{\dot{u}^f\}_L + ([G_C]_R + [C]_R)\{\dot{u}^f\}_R
\end{aligned} \tag{2.2}$$

where

$[M]$, $[C]$, $[K]$, in order, are the mass matrix, damping matrix and stiffness matrix.

$\{u\}$, $\{\dot{u}\}$ and $\{\ddot{u}\}$ are the nodal displacement, velocity and acceleration vectors respectively.

$[C]_i$ ($i = BS, FR, BA, L, R$) is the viscous boundary matrix, which is aimed at absorbing the energy of the scattered waves in the foundation. The subscripts BS, FR, BA, L, R indicate the boundary position shown in Fig. 2.2.

$\{\dot{z}\}$ is the velocity vector of the ground earthquake motion (2E component).

$[G]_i$ ($i = FR, BA, L, R$) is the stiffness matrix, which is used for calculating the traction force acting on the lateral boundaries due to the displacement of the free fields.

$[G_c]_i$ ($i = FR, BA, L, R$) is the damping matrix, which is directly proportionate to the $[G]_i$ and is used for calculating the traction force acting on the lateral boundaries due to the velocity difference between the foundation and the free fields.

$\{u^f\}_i$, $\{\dot{u}^f\}_i$ and $\{\ddot{u}^f\}_i$ ($i = FR, BA, L, R$) are the displacement, velocity and acceleration vectors of the free fields.

However, for the model with fixed bottom boundary, the matrix $[C]_{BS}$ in Eqn. 2.2 becomes unnecessary, and the first term of the right side becomes

$$-[M]\{\ddot{z}\}$$

where $\{\ddot{z}\}$ is the acceleration vector of the ground earthquake motion (E+F component).

The bottom boundary condition of the free fields should be consistent with that of the foundation. For the case with bottom viscous boundary, the motion equation of the free fields should be

$$\left[M^f \right] \{\ddot{u}^f\} + \left(\left[C^f \right] + \left[C^f \right]_{BS} \right) \{\dot{u}^f\} + \left[K^f \right] \{u^f\} = \left[C^f \right]_{BS} \{\dot{z}^f\} \quad (2.3)$$

where $\left[K^f \right]$ is the stiffness matrix of the free field. It can be achieved by superposition of the elemental matrices. Corresponding to the excitation direction, the elemental matrix has different contents as shown in Eqn. 2.4.

$$\left[K^f \right]^e = \begin{cases} \frac{\mu}{H} \begin{bmatrix} 1 & -1 \\ -1 & 1 \end{bmatrix} & \text{horizontal excitation} \\ \frac{\lambda + 2\mu}{H} \begin{bmatrix} 1 & -1 \\ -1 & 1 \end{bmatrix} & \text{vertical excitation} \end{cases} \quad (2.4)$$

where μ is the shear elastic modulus of the free field material.

$\lambda = 2\mu\nu/(1-2\nu)$, and ν is the Poisson ratio.

H is the thickness of the layer element of the free field.

While, $\left[M^f \right]$ in Eqn. 2.3 is the mass matrix of the free field, and

$\left[C^f \right]$ is the damping matrix, which is proportional to $\left[K^f \right]$ and $\left[M^f \right]$.

$\{\dot{z}^f\}$ is the velocity vector of the ground motion, and

$\left[C^f \right]_{BS}$ is the matrix of the bottom viscous boundary of the free fields, which is defined by corresponding to the excitation direction as Eqn. 2.5 does.

$$\left[C^f \right]_{BS} = \begin{cases} \begin{bmatrix} 0, 0, \dots, \rho V_s \end{bmatrix} & \text{horizontal excitation} \\ \begin{bmatrix} 0, 0, \dots, \rho V_p \end{bmatrix} & \text{vertical excitation} \end{cases} \quad (2.5)$$

When the bottom boundary of the free field is fixed, the right side of Eqn. 2.3 becomes

$$-\left[M^f \right] \{\ddot{z}^f\}$$

where $\{\ddot{z}^f\}$ is the acceleration vector of the ground earthquake motion.

3. 3-D EXTENSION OF THE STIFFNESS MATRICES OF THE LATERAL BOUNDARIES CONSIDERING THE EFFECT OF THE VERTICAL MOTION

Around the foundation of the numerical model, the lateral viscous boundaries are set, which consist of 3-D springs and dampers as shown in Fig.3.1. It is supposed that 3 directional ground motions are input.

The artificial lateral boundary should have the function of not only to absorb the energy of the scattered waves occurred in the system but also to let the energy of the free field motion flow into the foundation simultaneously. The effect of the free fields is expressed as traction force as shown in Fig.3.2. The inflow energy can be classified into two types. One is due to the displacement of the free

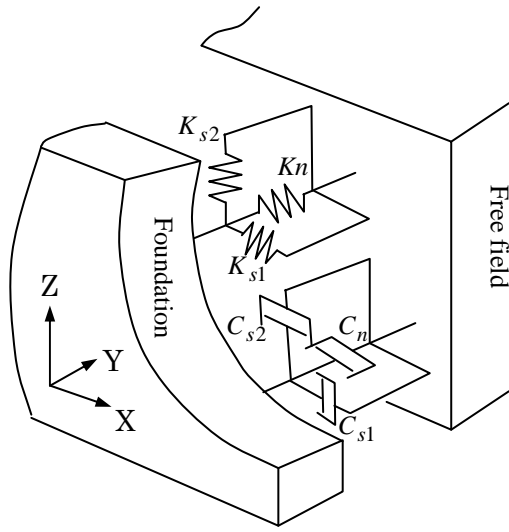


Figure 3.1 Extension of lateral boundary matrix

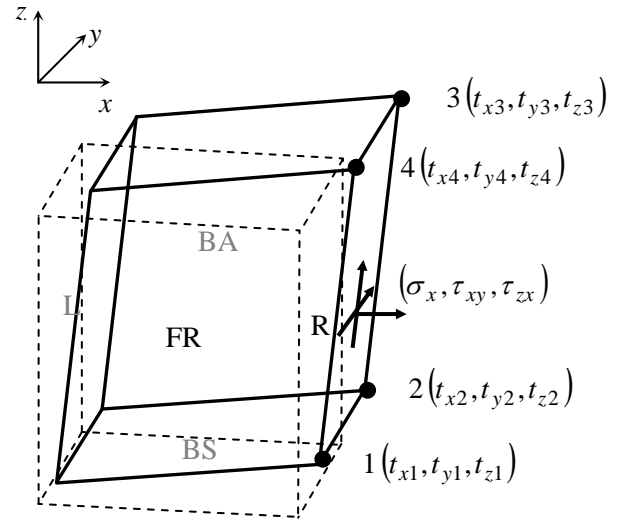


Figure 3.2 Traction on the boundary surface

field, expressed as $\{f_d^f\}$, and the other is due to the velocity difference between the foundation and the free fields, which is expressed as $\{f_v^f\}$. Therefore, the traction force acting on the lateral boundary surface can be defined as

$$\{f^f\} = \{f_d^f\} + \{f_v^f\} \quad (3.1)$$

where, $\{f^f\}$, as shown in Fig.3.2, consist of the nodal forces

$$\{f^f\} = \{t_{x1} \ t_{y1} \ t_{z1} \ t_{x2} \ \cdots \ t_{x4} \ t_{y4} \ t_{z4}\}^T \quad (3.2)$$

In the original paper of Miura, the method for calculating the traction force acting on the lateral boundaries in the case of single exciting direction was given. Here, the method is improved to correspond to the 3 directional vibration problems. The first term of Eqn. 3.1 is described as a 3 - dimensional problem.

With the same derivation method as Miura did, the traction forces acting on the lateral boundaries due to the displacement of the free field can be expressed as

$$\{f_d^f\}_i = [G]_i^e \{u^f\}^T \quad (i = FR, BA, L, R) \quad (3.3)$$

For example, corresponding to the right side boundary R as shown in the Fig.3.2, in the case of three directional deformation problems, the displacement vector of the connecting free field $\{u^f\}$ is defined as

$$\{u^f\} = \{u_1 \ v_1 \ w_1 \ u_2 \ \cdots \ \cdots \ u_4 \ v_4 \ w_4\}^T \quad (3.4)$$

On the other hand, the elemental stiffness matrix of the right side boundary is defined as

$$[G]_R^e = \begin{bmatrix} 0 & 0 & -\theta & 0 & 0 & -\theta & 0 & 0 & \theta & 0 & 0 & \theta \\ 0 & 0 & 0 & 0 & 0 & 0 & 0 & 0 & 0 & 0 & 0 & 0 \\ -\phi & 0 & 0 & -\phi & 0 & 0 & \phi & 0 & 0 & \phi & 0 & 0 \\ 0 & 0 & -\theta & 0 & 0 & -\theta & 0 & 0 & \theta & 0 & 0 & \theta \\ 0 & 0 & 0 & 0 & 0 & 0 & 0 & 0 & 0 & 0 & 0 & 0 \\ -\phi & 0 & 0 & -\phi & 0 & 0 & \phi & 0 & 0 & \phi & 0 & 0 \\ 0 & 0 & -\theta & 0 & 0 & -\theta & 0 & 0 & \theta & 0 & 0 & \theta \\ 0 & 0 & 0 & 0 & 0 & 0 & 0 & 0 & 0 & 0 & 0 & 0 \\ -\phi & 0 & 0 & -\phi & 0 & 0 & \phi & 0 & 0 & \phi & 0 & 0 \\ 0 & 0 & -\theta & 0 & 0 & -\theta & 0 & 0 & \theta & 0 & 0 & \theta \\ 0 & 0 & 0 & 0 & 0 & 0 & 0 & 0 & 0 & 0 & 0 & 0 \\ -\phi & 0 & 0 & -\phi & 0 & 0 & \phi & 0 & 0 & \phi & 0 & 0 \end{bmatrix} \quad (3.5)$$

where,

$$\begin{cases} \phi = \frac{\mu \cdot d}{8} \\ \theta = \frac{\lambda \cdot d}{8} \end{cases} \quad \text{while } d \text{ indicates the size shown in Fig.2.2.}$$

For the left side boundary L, the elemental stiffness matrix can be achieved according to the position relationship with the right side boundary.

$$[G]_L^e = -[G]_R^e \quad (3.6)$$

In the same way, the elemental stiffness matrix of the front side boundary FR can be defined as

$$[G]_{FR}^e = \begin{bmatrix} 0 & 0 & 0 & 0 & 0 & 0 & 0 & 0 & 0 & 0 & 0 & 0 \\ 0 & 0 & \eta & 0 & 0 & \eta & 0 & 0 & -\eta & 0 & 0 & -\eta \\ 0 & \zeta & 0 & 0 & \zeta & 0 & 0 & -\zeta & 0 & 0 & -\zeta & 0 \\ 0 & 0 & 0 & 0 & 0 & 0 & 0 & 0 & 0 & 0 & 0 & 0 \\ 0 & 0 & \eta & 0 & 0 & \eta & 0 & 0 & -\mu & 0 & 0 & -\eta \\ 0 & \zeta & 0 & 0 & \zeta & 0 & 0 & -\zeta & 0 & 0 & -\zeta & 0 \\ 0 & 0 & 0 & 0 & 0 & 0 & 0 & 0 & 0 & 0 & 0 & 0 \\ 0 & 0 & \eta & 0 & 0 & \eta & 0 & 0 & -\eta & 0 & 0 & -\eta \\ 0 & \xi & 0 & 0 & \zeta & 0 & 0 & -\zeta & 0 & 0 & -\zeta & 0 \\ 0 & 0 & 0 & 0 & 0 & 0 & 0 & 0 & 0 & 0 & 0 & 0 \\ 0 & 0 & \eta & 0 & 0 & \eta & 0 & 0 & -\eta & 0 & 0 & -\eta \\ 0 & \zeta & 0 & 0 & \zeta & 0 & 0 & -\zeta & 0 & 0 & -\zeta & 0 \end{bmatrix} \quad (3.7)$$

where

$$\begin{cases} \zeta = \frac{\mu \cdot l}{8} \\ \eta = \frac{\lambda \cdot l}{8} \end{cases} \quad \text{while } l \text{ indicates the size shown in Fig.2.2.}$$

And the elemental stiffness matrix of the back side boundary can be achieved from the Eqn. 3.8.

$$[G]_{BA}^e = -[G]_{FR}^e \quad (3.8)$$

The equations from Eqn. 3.5 to Eqn. 3.8 are the ones that belong to the boundary elements. For each boundary FR, BA, L, R, the total stiffness matrices of the boundaries can be achieved by the combination of the above elemental stiffness matrices.

4. VERIFICATION OF THE IMPROVED VISCOUS BOUNDARY CONDITION

A laterally layered ground is analyzed to verify the function of the viscous boundary conditions improved in the study. For verification of the lateral boundaries, the 3-D analysis of a program called "UNIVERSE", which has the function of the improved viscous boundary, is compared with that of the 1-D program "SHAKE". For three dimensional analyses, a proper set of boundary conditions should be that which has the function of not only absorbing the internal scattered waves but also transmitting the energy resulted from the motion of the free field into the foundation. It is assumed that for a dynamic analysis of the layered ground, if the boundary conditions are properly set, the results gotten from the 3-D analysis with limited region should be consistent with those of the 1-D analysis of SHAKE. For verification of the bottom boundary, the horizontal and vertical earthquake motions are input simultaneously, and the responses of the foundation are compared with those of the free fields around the foundation.

4.1. Verification Conditions

The verification analyses are carried out with the model shown in Fig.4.1.

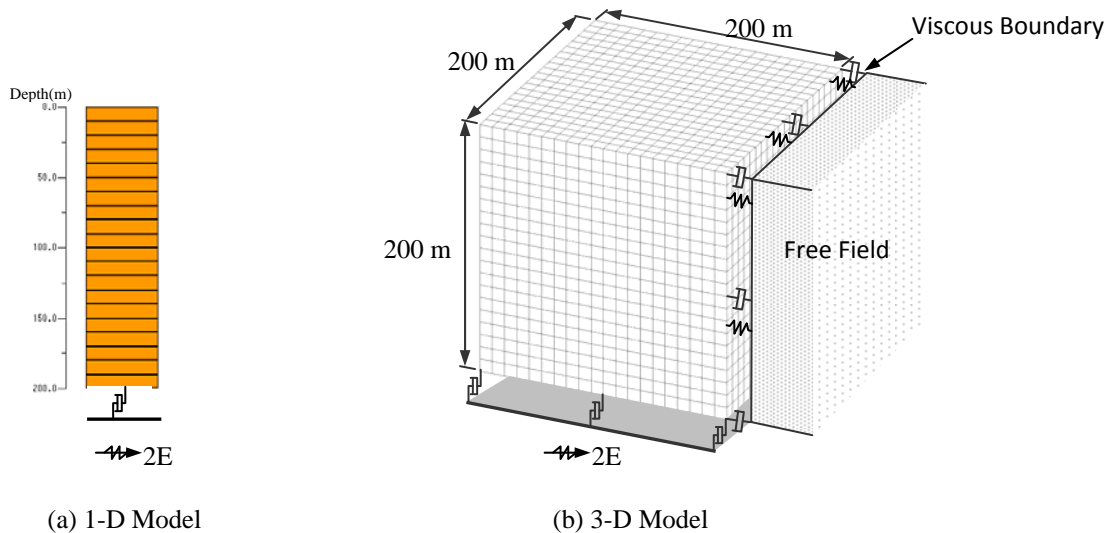


Figure 4.1 Model for verification analysis

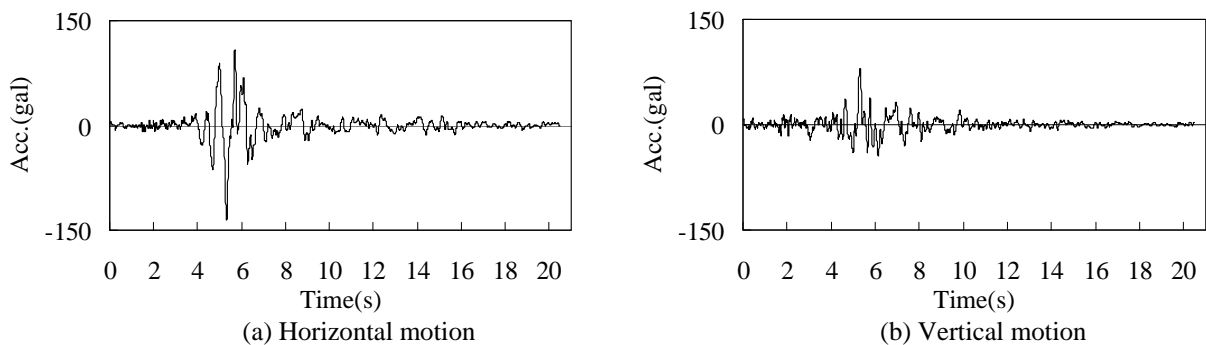


Figure 4.2 Input waves

The material properties of both the 1-D model and the 3-D model are exactly the same. It is supposed to be linear elastic material and the properties shown in Table 4.1 are used.

Table 4.1 Material Properties of the Model

Elastic Modulus(N/mm ²)	Density (g/cm ³)	Poisson Ratio	Damping Coefficient
20000.00	2.60	0.30	0.05

The input waves beneath the bottom viscous boundary are shown in Fig.4.2, which are the earthquake records at a dam site during the Hyogo-ken Nanbu earthquake in 1995.

4.2. Analytic Results

4.2.1. Function of lateral boundary

Fig.4.3 shows the distribution of the maximum acceleration response. It is clear that the artificial lateral boundary has no effect on the acceleration response of the model. In other words, the lateral boundary condition acted perfectly in the analysis. It can be also confirmed by Fig.4.4, which shows the acceleration histories of the typical points and the maximum distribution in depth.

Table 4.2 compares the maximum acceleration response of the program UNIVERSE and SHAKE. The maximum relative error is 2.96%, which is assumed to be due to the difference between the FEM solution and the theoretic solution. Fig.4.5 shows the acceleration response histories and the Fourier spectrums achieved by the two programs.

From these results it can be identified that the 3-dimensional analysis with the artificial boundary conditions gives almost the same results of the 1-dimensinal analysis. This indicates that the boundary conditions proposed in the study act quite well in the 3-dimensional analysis.

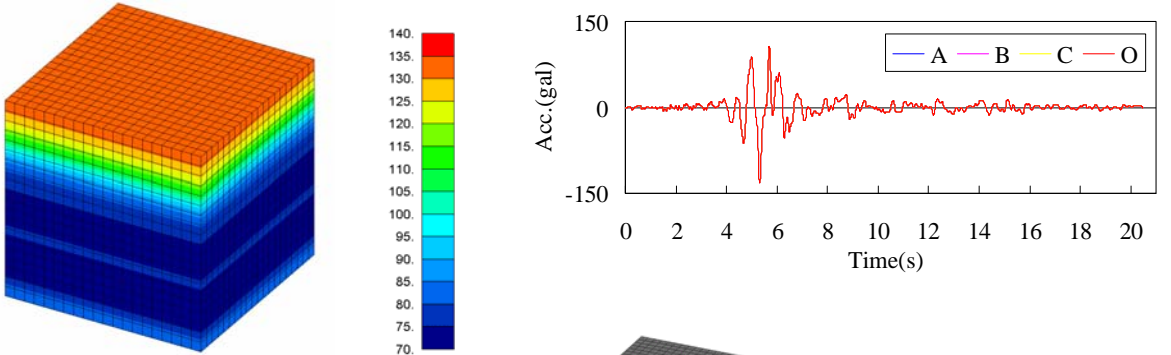


Figure 4.3 Maximum acceleration

Table 4.2 Comparison of the Maximum Acceleration Between UNIVERSE and SHAKE

Position	UNIVERSE (gal)	SHAKE (gal)	Relative Error (%)
Centre of the surface	132	135	1.92
Centre of the model	71	73	2.96
Centre of the bottom	86	88	2.48

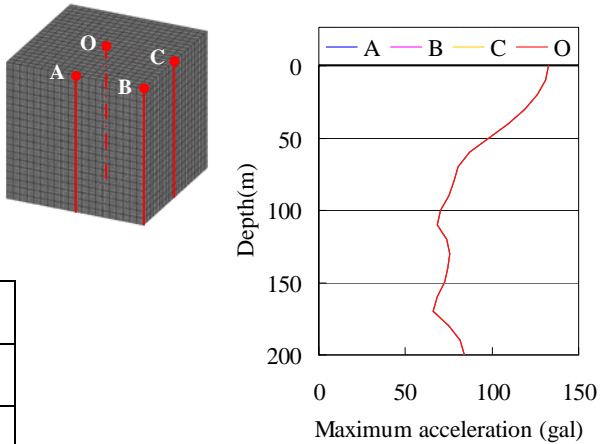


Figure 4.4 Acceleration response

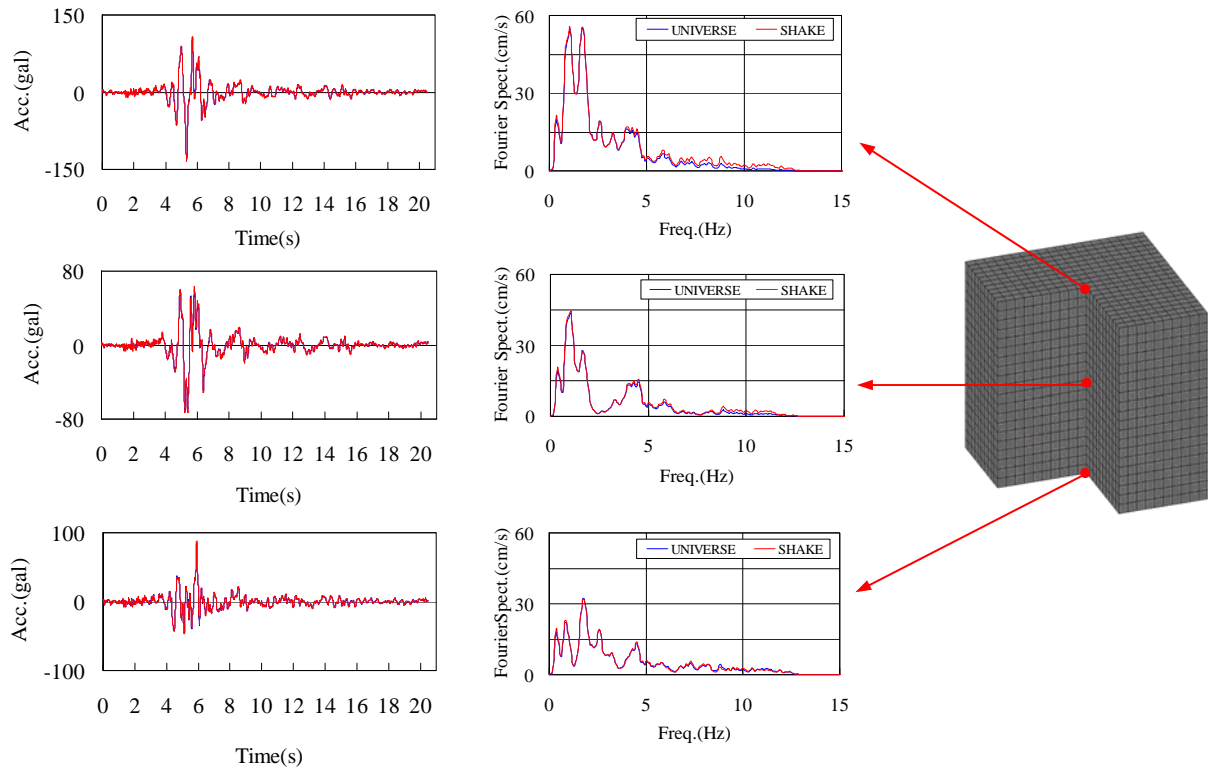


Figure 4.5 Comparison of acceleration response history and Fourier spectrums

4.2.2. Function of bottom boundary

With the same analytic conditions mentioned in the section 4.1, but the horizontal and vertical earthquake motions are inputted simultaneously from the surface under the bottom viscous boundary. The displacement responses are examined, although the acceleration, velocity, stress responses etc. are also output. It was thought that if the bottom viscous boundary is properly set, the responses of the ground should be consistent with those of the free field around the ground.

Fig.4.6 shows the displacement responses of the specified positions and those of the free field around the ground. It is clear that the motions of the ground and the free field are completely consistent in both horizontal and vertical directions. It means that both the bottom and lateral boundary conditions functioned properly.

5. CONCLUSION

In this study the viscous boundary condition based on the principle of virtual work has been improved for considering the effects of vertical earthquake motion.

The FEM formulation of the motion equation of the foundation - structure system, when the bottom viscous boundary is applied, has been presented, and the earthquake input formation is also given. The stiffness matrix for calculating the traction acting on the lateral boundary of the foundation due to the free field motion is modified for corresponding to the three dimensional earthquake motions. Therefore, the energy due to the free field motion can flow into the foundation naturally. Compared with the original proposal given by Miura, the earthquake responses can be achieved with higher precision even when the bottom viscous boundary condition is used. With the method proposed in the study the scattered waves, especially the reflection in the vertical direction at the foundation bottom can be averted and an accurate solution can be expected.

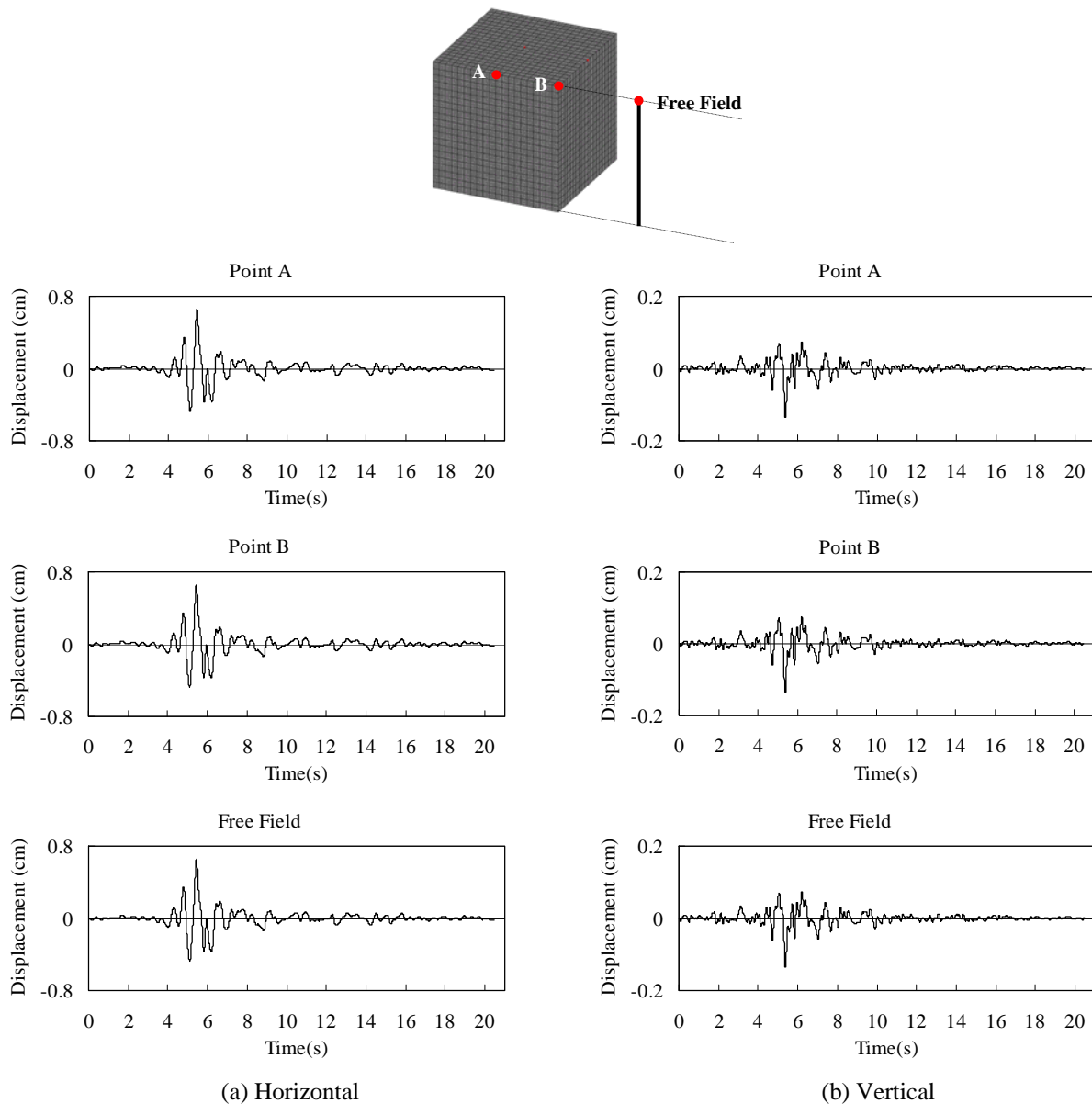


Figure 4.6 Displacement response of typical points and free field when subject to the horizontal and vertical earthquake motion simultaneously

ACKNOWLEDGEMENT

We are deeply grateful to Prof. Watanabe H., former professor of Saitama University, Japan for his long years of dedicated instruction. We would like to express an acknowledgment to Prof. Miura F., Yamaguchi University, Japan for his kind guidance for this study, and we want to thank Dr. Sasaki T., Japan Dam Engineering Centre for his suggestions and cooperation throughout the study.

REFERENCES

- Miura, F., Okinaka, H. (1989). Dynamic Analysis Method for 3-D Soil-Structure Interaction Systems With the Viscous Boundary Based on the Principle of Virtual Work. *Journal of Structural Mechanics and Earthquake Engineering, JSCE, No.404/I-11*, 395-404
- Lysmer, J. and Waas, G. (1972). Shear waves in plane infinite structure, *Proc. of ASCE, Vol.98*, 85-105
- Schnabel, P. B., Lysmer, J. and Seed, H. B. (1975). SHAKE a computer program for earthquake response analysis of horizontally layered sites, Report No. **EERC75-30**, University of California, Berkeley